J Fluoresc
DOI 10.1007/s10895-015-1700-4

ORIGINAL ARTICLE

Symmetric *Meso*-Chloro-Substituted Pentamethine Cyanine Dyes Containing Benzothiazolyl/Benzoselenazolyl Chromophores Novel Synthetic Approach and Studies on Photophysical Properties upon Interaction with bio-Objects

Atanas Kurutos[1] · **Olga Ryzhova**[2] · **Valeriya Trusova**[2,3] · **Galyna Gorbenko**[2] · **Nikolay Gadjev**[1] · **Todor Deligeorgiev**[1]

Received: 19 June 2015 / Accepted: 20 October 2015

Abstract A series of symmetric pentamethine cyanine dyes derived from various N-substituted benzothiazolium/benzoselenazolium salts, and a conjugated bis-aniline derivative containing a chlorine atom at *meso*-position with respect to the polymethine chain, were synthesized using a novel improved synthetic approach under mild conditions at room temperature. The reaction procedure was held by grinding the starting compounds for relative short times. The novel method is reliable and highly reproducible. Some photophysical characteristics were recorded in various solvents, including absorption, and fluorescence quantum yields using Cy-5 as a reference. Additional studies on interactions with several bio-objects such as liposomes, DNA, and proteins have been investigated in the present work.

Keywords Pentamethine cyanine dyes · 2-methylbenzothiazole · 2-methylbenzoselenazole · Fluorescent markers · Liposomes · DNA, proteins · H-aggregates

✉ Atanas Kurutos
ohtak@chem.uni-sofia.bg

✉ Valeriya Trusova
valtrusova@yahoo.com

[1] Sofia University "St. Kliment Ohridski", Faculty of Chemistry and Pharmacy, 1, blv. J. Bourchier, 1164 Sofia, Bulgaria

[2] Department of Nuclear and Medical Physics, V.N. Karazin Kharkiv National University, 4 Svobody Sq., Kharkiv 61077, Ukraine

[3] 19-32 Geroyev Truda, Kharkiv 61044, Ukraine

Introduction

Cyanine dyes, a wide class of fluorescent probes with unique photophysical properties, have found numerous application in different areas as optical imaging agents [1, 2], active ingredients in semiconducting materials [3, 4], laser dyes [5], photographic sensitizers [6, 7], photopolymerization initiators [8, 9], stains and fluorescent labels [10–13], to name only a few. These compounds are of particular interest for biomedical research and diagnostics due to their favorable spectral characteristics, namely, longwave absorption and emission, large extinction coefficient, high fluorescence quantum yield, etc. Most of the cyanine dyes are photosensitive compounds possessing two quaternized, nitrogen-containing, heterocyclic structures, which are linked through a polymethine bridge [14]. Due to dual hydrophobic and cationic nature of these dyes, which leads to strong interaction with polyanionic DNA duplex, cyanines are mainly used as bright labels for nucleic acids in microarray-based expression analysis [15], DNA sequencing [16, 17] and DNA intercalation bioanalytical assays [18]. It has been demonstrated that mono-, tri- and pentamethine cyanine dyes are suitable for quantitative detection of amyloid formation and protein labeling [19, 20]. Fluorescence intensity of cyanine dyes is greatly increased upon their binding to nucleic acids or proteins as a result of the rigidization of the fluorophores [19–22]. Furthermore, the utility of near infrared cyanine dyes demonstrates unique hydrophobic characteristics in aqueous medium that were exploited for target-specific pH probing [23, 24]. Moreover, it is known that the central polymethine chain of

Published online: 02 November 2015

cyanine dyes can be cleaved by reactive oxygen and nitrogen species, which gives the impetus for cyanine use for in vivo sensing of oxidative stress and monitoring the dynamics of redox cycles in living cells [25]. In addition, cyanine dyes showed unique properties as optical imaging probes for cancer labeling [26].

Despite the essential utility and versatility of cyanines, significant research efforts are being directed at the developing and investigating new fluorescent compounds. The present paper is aimed at the synthesis and characterization of a range of symmetric pentamethine dyes differing in their structural features and spectroscopic behaviour. More specifically, our goals were: (i) to synthesize a series of symmetric pentamethine fluorophores containing a benzothiazolic and benzoselenazolic heterocycle with a *meso*-chlorine substituent in the polymethine chain; (ii) to characterize their photophysical properties; (iii) to explore possible biological applications of cyanine analogues.

Experimental

Materials

All starting materials and solvents required for the synthesis of the dyes were purchased from Sigma-Aldrich, Organica, Fluka, Alfa-Aesar, Deutero GmBH. The structures of all intermediates are evaluated on the final products. The target cyanine dyes were recrystallized from methanol and characterized by ^{1}H NMR spectra recorded on a Brucker Avance III HD, 500 MHz in DMSO-d_6 at 25 °C. The chemical shifts were reported in ppm in δ-values with respect to tetramethylsilane (TMS) as an internal standard or the deuterated solvent peak. Coupling constants J are expressed in Hz. The melting points were determined on a Kofler apparatus and are uncorrected. Bovine heart cardiolipin (CL) and 1-palmitoyl-2-oleoyl-*sn*-glycero-3-phosphocholine (PC) were from Avanti Polar Lipids (Alabaster, AL). Cattle spleen DNA was from Reakhim (Russia), bovine serum albumin (BSA) and Tris-HCl were obtained from Sigma. 4-(dimethylaminostyryl)-1-dodecylpiridine n-toluenesulfonate (DSP-12) was purchased from Zonde (Latvia). All other starting materials and solvents were commercial products of analytical grade and were used without further purification.

Preparation of Pentamethine dye Intermediates 2a, 2b

2-methylbenzoselenazole **1a**/2-methylbenzothiazole **1b** (5 mmol) was dissolved in 10 ml acetone in an Erlenmeyer flask, to which dimethyl sulfate (5.5 mmol) was added dropwise. Upon completion of the addition, the resulting mixture was stored in a dark, closed vessel at room temperature for 48 hours (Scheme 1). The corresponding quaternary benzazolium salt precipitate was collected on a Buchner and

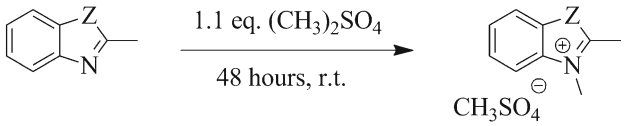

1a-1b **2a-2b**

Z = S, Se

Scheme 1 Synthesis of 2,3-dimethyl benzothiazolium and 2,3-dimethylbenzselenazolium salts **2a-2b**

stored in a dessicator. The compounds **2a-2b** were used without further purification in the next reaction steps for obtaining the pentamethine dyes. Their structures are evaluated on the final products. Yields: 2,3-dimethylbenzothiazolium methosulfate **2a** = 87 %, 2,3-dimethylbenzselenazolium methosulfate **2b** = 83 %.

Preparation of N-Quaternary 2-Methyl Benzothiazolium and 2-Methylbenzselenazolium Salts 2c-2g

2-methylbenzoselenazole/2-methylbenzothiazole **1a,1b** (5 mmol) and the corresponding alkylating agent **R-X** (5.5 mmol) were mixed together in a 50 ml Erlenmeyer flask with 10 ml 2-methoxyethanol and the mixture was refluxed for 2 hours with stirring (Scheme 2). Upon completion, the mixture was left to cool down to room temperature, followed by addition of 20–30 ml diethyl ether to it, in order to precipitate the desired products. The quaternary salts were suction filtered and stored in a dessicator. The compounds were used without further purification in the next reaction steps for obtaining the pentamethine dyes. Their structures were evaluated on the final products (Scheme 3). Chemical structures of the quaternary benzazolium salts **2c-2g** are presented in Table 1.

Synthesis of Pentamethine Cyanine Dyes AK5 by an Improved Method

Substituted or unsubstituted 2-methylbenzothiazolium/2-methylbenzoselenazolium quaternary salts **2a-2g** (3 mmol) and ((2-chloro-3-(phenylamino)allylidene)benzenaminium chloride)) **3** (1.5 mmol), were mixed together with 5 ml

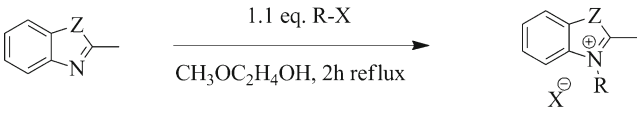

1a-1b **2c-2g**

Z = S, Se
R = C_2H_5, $C_6H_5CH_2$, C_2H_4CN, C_2H_4OH
X = Br, I

Scheme 2 Synthesis of N-quaternary 2-methyl benzothiazolium and 2-methylbenzselenazolium salts **2c-2g**

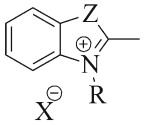

2a-2g

Z = S, Se
R = CH_3, C_2H_5, $C_6H_5CH_2$, C_2H_4CN, C_2H_4OH
X = CH_3SO_4, Br, I

Scheme 3 Chemical structures of the quaternary benzazolium salts **2a-2g**

methanol in a mortar with a pestle (Scheme 4). As soon as the mixture becomes homogeneous, anhydrous sodium acetate (3 mmol) was added upon grinding at room temperature. Usually, a dark blue color is spontaneously developed, which indicates the formation of the target polymethine cyanine dye **5** (Scheme 5)**.** In addition to, the mixture crystalizes almost straight forward. The reaction is also monitored by TLC. Upon completion, (it usually takes few minutes) the product was dissolved in methanol and transferred to a beaker containing 200 ml of an aqueous solution of potassium iodide. The precipitated dye was suction filtered and air dried. All yield calculations were made to the crude products. Their purification was held by recrystallization from methanol. The structures of the pentamethine cyanine dyes **AK5** were evaluated by ^{1}H NMR spectroscopy (see Experimental section).

Analysis Methods and Equipment

^{1}H NMR spectra were recorded on a Bruker Avance III 500MHz instrument in DMSO-d6. Melting points were determined on a Köfler apparatus and are uncorrected.

AK5-1 ***2-((1E,3Z,5E)- 3-chloro-5-(3-methylbenzo[d]thiazol-2(3 H)-ylidene)penta-1,3-dien-1-yl)-3-methylbenzo[d]thiazol-3-ium iodide*** (Yield of crude product 96 %, M.p. = 255–257 °C); UV/VIS (methanol): λmax =645 nm, ε = 204.000 l.mol^{-1}.cm$^{-1,}$ λem = 660 nm, Q = 0.10; ^{1}H NMR (500 MHz; DMSO d_6) δ (ppm): 3.90 (s, 6 H, 2 x CH_3-N); 6.39 (d, J 13.0, 2 H, 2 x CH); 7.44 (m, 2 H, ArH.); 7.60 (m, 2 H, ArH.); 7.80 (d, J 8.3; 2 H, ArH.); 8.03 (d, J 13.1, 2 H, 2 x CH); 8.06 (d, J 7.9, 2 H, ArH.);

Table 1 Chemical structures of the quaternary benzazolium salts

Compound	Z	R	X	Yield (%)	m.p. (°C)
2a	S	CH_3	CH_3SO_4	87	143–145
2b	Se			83	*
2c	S	C_2H_5	I	74	193–195
2d	Se			67	*
2e	S	C_2H_4CN	Br	63	248–249
2f		C_2H_4OH		91	*
2g		$C_6H_5CH_2$		72	224–227

*Products 2b, 2d, 2f were found to be hygroscopic, so melting points could not be determined

AK5-2 ***2-((1E,3Z,5E)- 3-chloro-5-(3-methylbenzo[d][1,3]selenazol-2(3 H)-ylidene)penta-1,3-dien-1-yl)-3-methylbenzo[d][1,3]selenazol-3-ium iodide*** (Yield of crude product 94 %, M.p. = 255–258 °C); UV/VIS (methanol): λmax =655 nm, ε = 229.000 l.mol^{-1}.cm^{-1}, λem = 672 nm, Q = 0.081; ^{1}H NMR (500 MHz; DMSO d_6) δ (ppm): 3.87 (s, 6 H, 2 x CH_3-N); 6.52 (d, J 12.9, 2 H, 2 x CH); 7.38 (m, 2 H, ArH.); 7.57 (m, 2 H, ArH.); 7.75 (d, J 8.1; 2 H, ArH.); 8.00 (d, J 12.8, 2 H, 2 x CH); 8.13 (dd, J 0.9, 7.9, 2 H, ArH.);

AK5-3 ***2-((1E,3Z,5E)- 3-chloro-5-(3-ethylbenzo[d]-thiazol-2(3 H)-ylidene)penta-1,3-dien-1-yl)-3-ethylbenzo[d]-thiazol-3-ium iodide*** (Yield of crude product 98 %, M.p. = 251–253 °C); UV/VIS (methanol): λmax =646 nm, ε = 266.000 l.mol^{-1}.cm^{-1}, λem = 660 nm, Q = 0.10; ^{1}H NMR (500 MHz; DMSO d_6) δ (ppm): 1.35 (t, J 7.1, 6 H, 2 x CH_3-CH_2); 4.48 (q, J 6.9, 4 H, 2 x CH_3-CH_2-N); 6.40 (d, J 13.1, 2 H, 2 x CH); 7.46 (m, 2 H, ArH.); 7.60 (m, 2 H, ArH.); 7.83 (d, J 8.3; 2 H, ArH.); 8.07 (d, J 13.0, 2 H, 2 x CH); 8.08 (d, J 7.5, 2 H, ArH.);

AK5-4 ***2-((1E,3Z,5E)- 3-chloro-5-(3-ethylbenzo[d][1,3]selenazol-2(3 H)-ylidene)penta-1,3-dien-1-yl)-3-ethylbenzo[d][1,3]selenazol-3-ium iodide*** (Yield of crude product 95 %, M.p. = 241–243 °C); UV/VIS (methanol): λmax =657 nm, ε = 254.000 l.mol^{-1}.cm^{-1}, λem = 673 nm, Q = 0.07; ^{1}H NMR (500 MHz; DMSO d_6) δ (ppm): 1.34 (t, J 7.2, 6 H, 2 x CH_3-CH_2); 4.46 (q, J 7.1, 4 H, 2 x CH_3-CH_2-N); 6.53 (d, J 12.8, 2 H, 2 x CH); 7.40 (m, 2 H, ArH.); 7.58 (m, 2 H, ArH.); 7.78 (d, J 8.3; 2 H, ArH.); 8.04 (d, J 12.8, 2 H, 2 x CH); 8.15 (d, J 1.1, 7.9, 2 H, ArH.);

AK5-6 ***2-((1E,3Z,5E)- 3-benzyl-5-(3-benzylbenzo[d]-thiazol-2(3 H)-ylidene)-3-chloropenta-1,3-dien-1-yl)benzo[d]thiazol-3-ium iodide*** (Yield of crude product 99 %, M.p. = 224–227 °C); UV/VIS (methanol): λmax =653 nm, ε = 219.000 l.mol^{-1}.cm^{-1}, λem = 669 nm, Q = 0.13; ^{1}H NMR (500 MHz; DMSO d_6) δ (ppm): 5.76 (s, 4 H, 2 x CH_2-N); 6.45 (d, J 13.1, 2 H, 2 x CH); 7.25 (d, J 7.4, 4 H, ArH.); 7.33 (d, J 7.2, 2 H, ArH.); 7.37–7.40 (m, 4 H, ArH.); 7.47 (m, 2 H, ArH.); 7.58 (m, 2 H, ArH.); 7.83 (d, J 8.4; 2 H, ArH.); 8.06 (d, J 13.0, 2 H, 2 x CH); 8.12 (d, J 7.98, 2 H, ArH.);

AK5-8 ***2-((1E,3Z,5E)- 3-chloro-5-(3-(2-cyanoethyl)-benzo[d]thiazol-2(3 H)-ylidene)penta-1,3-dien-1-yl)-3-(2-cyanoethyl)benzo[d]thiazol-3-ium iodide*** (Yield of crude product 39 %, M.p. = 276–277 °C); UV/VIS (methanol): λmax =652 nm, ε = 273.000 l.mol^{-1}.cm^{-1}, λem = 670 nm, Q = 0.08; ^{1}H NMR (500 MHz; DMSO d_6) δ (ppm): 3.12 (t, J, 6.5; 2 H, CH_2-CN); 4.83 (t, J 6.5, 4 H, 2 x CH_2-N); 6.58 (d, J 13.0, 2 H, 2 x CH); 7.48 (m, 2 H, ArH.); 7.62 (m, 2 H, ArH.); 7.91 (d, J 8.3; 2 H, ArH.); 8.09 (dd, J 0.9, 7.9, 2 H, ArH.); 8.11 (d, J 12.9, 2 H, 2 x CH);

Scheme 4 Synthetic approach for the synthesis of dyes **AK5**

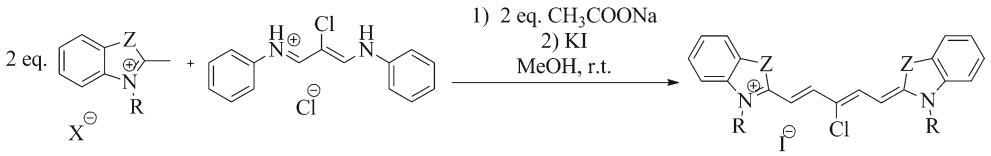

2a-2g **3** **AK5 dyes**

Z = S, Se
R = CH_3, C_2H_5, $C_6H_5CH_2$, C_2H_4CN, C_2H_4OH
X = Br, I

AK5-9 ***2-((1E,3Z,5E)- 3-chloro-5-(3-(2-hydroxyethyl)-benzo[d]thiazol-2(3 H)-ylidene)penta-1,3-dien-1-yl)-3-(2-hydroxyethyl)benzo[d]thiazol-3-ium iodide*** (Yield of crude product 38 %, M.p. = 232–235 °C); UV/VIS (methanol): λmax =650 nm, ε = 278.000 l.mol^{-1}.cm^{-1}, λem = 666 nm, Q = 0.10; ^{1}H NMR (500 MHz; DMSO d_6) δ (ppm): 3.83 (q, J, 5.3; 4 H, CH_2-CH_2-OH); 4.51 (t, J 5.0, 4 H, 2 x CH_2-CH_2-N); 5.14 (t, J 5.6, 2 H, OH-CH_2); 6.50 (d, J 13.2, 2 H, 2 x CH); 7.44 (m, 2 H, ArH.); 7.57 (m, 2 H, ArH.); 7.89 (d, J 8.4; 2 H, ArH.) 8.02 (d, J 13.1, 2 H, 2 x CH); 8.06 (dd, J 0.9, 8.0, 2 H, ArH.);

Preparation of Working Solution

Stock solutions of cyanines were prepared immediately before the absorption or fluorescence measurements by dissolving the dyes in organic solvents. Stock solutions of DNA and BSA were prepared in 10 mM Tris-HCl buffer, pH 7.4. The concentrations of dyes, DNA and BSA were determined spectrophotometrically using their molar absorptivities and ε_{260}= 6.4×10^3M^{-1}cm^{-1}, ε_{276}=4.25×10^4M^{-1}cm^{-1} for DNA and BSA, respectively. The molar absorptivities of the dyes are given in Table 3. Working solution of cyanines were prepared by dilution of the dye stock solution in buffer. To determine the absorption of pentamethines in the presence of biomacromolecules and model membranes, appropriate amounts of the stock solution of DNA, BSA or liposomes were added to each dye in buffer.

Lipid vesicles composed of PC and PC mixtures with CL were prepared using the extrusion technique. A thin lipid film was first formed from the lipid mixtures in chloroform by removing the solvent under a stream of nitrogen. The dry lipid residues were subsequently hydrated with 20 mM HEPES, 0.1 mM EDTA, pH 7.4 at room temperature to yield lipid concentration of 1 mM. Thereafter, lipid suspension was extruded through a 100 nm pore size polycarbonate filter (Millipore, Bedford, USA). In this way, 3 types of lipid vesicles containing PC and 11 or 67 mol% CL were prepared, with the content of phosphate being identical for all liposome preparations. Hereafter, liposomes containing 11 or 67 mol% CL are denoted as CL11 or CL67, respectively. The phospholipid concentration was determined according to the procedure of Bartlett [27].

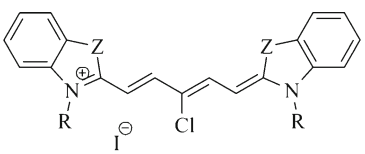

AK5 dyes

Z = S, Se
R = CH_3, C_2H_5, $C_6H_5CH_2$, C_2H_4CN, C_2H_4OH

Scheme 5 General structure of pentamethine cyanine dyes **AK5**

Fluorescence Measurements

The absorption and fluorescence spectra of pentamethines in organic solvents were recorded on a Cecil Aurius CE 3021 UV-Vis spectrophotometer and and Perkin Elmer LS45 spectrofluorimeter, respectively. The solvents used for the spectroscopic analyses were purchased form Macron Fine Chemicals TM. Absorption and fluorescence spectra of penthamethine dyes in the presence of liposomes, DNA and BSA were measured with CM2203 spectrophotometer at room temperature using 10-mm path-length quartz cuvettes.

The measurements of the Forster resonance energy transfer were performed using 4-(dimethylaminostyryl)-1-dodecylpiridine n-toluenesulfonate as an energy donor, with the excitation wavelength being 490 nm. Excitation and emission slit widths were set at 10 nm. Fluorescence intensity measured in the presence of pentamethine dyes at the maximum of DSP-12 emission was corrected for reabsorption and inner filter effects using the following coefficients [28]:

$$k_{\mathrm{corr}} = \frac{\left(1-10^{-A_0^{ex}}\right)\left(A_0^{ex}+A_a^{ex}\right)}{\left(1-10^{-\left(A_0^{ex}+A_a^{ex}\right)}\right)A_0^{ex}} \frac{\left(1-10^{-A_0^{em}}\right)\left(A_0^{em}+A_a^{em}\right)}{\left(1-10^{-\left(A_0^{em}+A_a^{em}\right)}\right)A_0^{em}} \quad (1)$$

where A_0^{ex}, A_0^{em} are the donor optical densities at the excitation and emission wavelengths in the absence of acceptor, A_a^{ex}, A_a^{em} are the acceptor optical densities at the excitation and emission wavelengths, respectively.

Quantum Yield Calculation

Quantum yields of the examined dyes were calculated using Cy5 as a standard according to the formula:

$$Q = \frac{Q_s\left(1-10^{-A_s}\right)S_p}{\left(1-10^{-A_p}\right)S_s}\cdot\frac{n_p^2}{n_s^2} \quad (1)$$

where Q_s is the standard quantum yield, $S_p$and S_s are the areas under the fluorescence spectra of the dye and standard, respectively, A_p and A_s are absorptions of the dye and standard at a certain excitation wavelength, n_p and n_s are refractive indexes of the measured dye solution and standard, respectively.

Results and Discussion

Synthesis and Structural Analysis of Pentamethine Dyes

A series of symmetric pentamethine cyanine dyes derived from various N-quaternary benzothiazolium/benzoselenazolium salts, and a conjugated bis-aniline derivative containing a chlorine atom at *meso*-position with respect to the polymethine chain, were synthesized using a novel synthetic approach using mild conditions at room temperature. The products were isolated with moderate to excellent yields as illustrated in (Table 2). Furthermore, the desired products obtained using the described procedure were evaluated by melting point temperatures, and ^{1}H NMR spectroscopy (see section 2).

Spectroscopic Characterization of Pentamethine Dyes in Different Organic Solvents and Buffer

As seen from Scheme 5, the cyanine dyes under investigation are symmetric pentamethine dyes containing a benzothiazolic and benzoselenazolic heterocycle with a *meso*-chlorine substituent with respect to the polymethine chain. Presented in Table 3 are the basic photophysical characteristics of the examined pentamethines in different organic solutions: absorption maximum (λ_A); molar absorptivities (ε) and emission maximum (λ_F). Absorption and fluorescence spectra of the dyes are typical for cyanines (Fig.1) with absorption maximum in DMSO in a range from 652 to 660 nm (monomeric dye form) and emission maxima from 670 to 682 nm depending on dye structure. A small shoulder in the absorption spectra around 600 nm corresponds to H-dimer formation [29]. It is well known that photophysical properties of cyanine dyes are directly influenced by the identity of the terminal heterocyclic groups and the length of polymethine chain [30]. Replacement of benzoselenazolic heterocycle instead of benzothiazolic one caused a 11 nm bathochromic shift in absorption and fluorescent maxima position for AK5-2 and AK5-4 in comparison with AK5-1 and AK5-3, respectively. Adding one methyl group to heterocyclic system of AK5-3 and AK5-4, resulted in no significant change in maxima position. Introduction of a phenyl ring, cyano and hydroxy group to AK5-6, AK5-8 and AK5-9 structure, respectively leads to 5–8 nm shift in absorption maximum positions compared to AK5-1. The Stocks shift of all compounds is approximately equal to 15–20 nm, that are typical for this class of dyes [31]. Upon varying the organic solvent polarity from DMSO to chloroform a 5–14 nm shift of absorption and fluorescence maximum positions was observed without any significant change in spectrum shape. Presented in Table 4 are the fluorescence quantum yield values of penthamethine cyanine dyes that were calculated using Cy5 as an internal standard. The dye AK5-6, containing phenyl ring displays the highest fluorescence quantum yield which is comparable with that of Cy5 (0.28 in DMSO). For all other studied dyes the quantum yields were in the range of 0.08–0.24 depending on dye structure and the organic solvents they were dissolved.

In an aqueous medium significant changes in cyanine spectral behavior were observed. Figure 2 represents the absorption spectra of the examined cyanine dyes in buffer solution. As judged from Fig. 2 and Table 5, the studied pentamethines, except of AK5-6, are characterized by broad spectrum in the range 500–700 nm with two well-defined peaks. The bathochromic one (ranging from 640 nm to 655 nm) corresponds to the absorption of monomeric dye species, while the hypsochromic one (with maximum between 583 nm and 596 nm) is a hallmark of H-aggregates. The ratio of these bands was found to depend on the dye chemical structure, but generally the monomer maximum prevailed over that of the aggregates. Furthermore, analysis of the absorption spectra of AK5-1 and AK5-2 showed that three instead of two bands are distinguished (low intensity maxima at 503 and 543 nm are appeared), which were attributed to the dye H-aggregates, H-dimers and monomers, respectively, starting from the left peak. In turn, AK5-6 exhibited a somewhat different behavior. More specifically, the absorption spectrum of this fluorophore was blue-shifted relative to the other dyes with the maximum centered around 542 nm. The monomer peak was virtually unstructured and resembled the spectrum shoulder, indicating

Table 2 Chemical structures of the pentamethine cyanine dyes

Dye	X	R	Yield (%)	melting point
AK5-1	S	CH_3	96	255–257
AK5-2	Se	CH_3	94	255–258
AK5-3	S	C_2H_5	98	251–253
AK5-4	Se	C_2H_5	95	241–243
AK5-6	S	$C_6H_5CH_2$	99	224–227
AK5-8	S	C_2H_4CN	39	276–277
AK5-9	S	C_2H_4OH	38	232–235

Table 3 Spectral characteristics of pentamethine cyanine dyes in different solutions

Dye	MeOH			DMSO			CH_3CN			DMF			$CHCl_3$		
	λmax (nm)	λem (nm)	ε ($x10^3$)	λmax (nm)	λem (nm)	ε ($x10^3$)	λmax (nm)	λem (nm)	ε ($x10^3$)	λmax (nm)	λem (nm)	ε ($x10^3$)	λmax (nm)	λem (nm)	ε ($x10^3$)
AK5-1	*645*	*660*	204	*652*	*670*	191	*643*	*659*	203	*649*	*667*	229	*659*	*676*	213
AK5-2	*655*	*672*	229	*663*	*681*	200	*654*	*672*	223	*660*	*678*	204	*673*	*687*	226
AK5-3	*646*	*660*	266	*652*	*671*	222	*644*	*661*	257	*650*	*667*	212	*659*	*676*	268
AK5-4	*657*	*673*	254	*665*	*682*	213	*655*	*673*	218	*662*	*679*	214	*673*	*687*	258
AK5-6	*653*	*669*	219	*660*	*678*	182	*651*	*669*	202	*657*	*675*	179	*667*	*683*	198
AK5-8	*652*	*670*	273	*660*	*679*	226	*651*	*669*	258	*657*	*676*	228	*665*	*684*	206
AK5-9	*650*	*666*	278	*657*	*676*	206	*648*	*666*	212	*654*	*672*	180	*664*	*681*	207

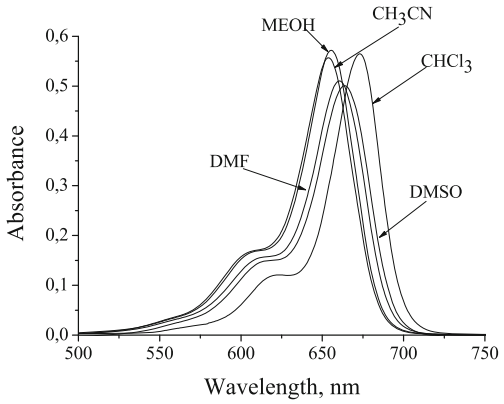

Fig. 1 Typical absorption spectra of pentamethine cyanine dyes in different organic solvents. AK5-2 concentration was 0.25 μM

that H-aggregates represent the dominating fraction of the dye molecules in buffer solution. It is known that the aggregation properties of cyanines are controlled by the balance between the van der Waals interactions, dispersion forces of the cyanine backbone, the forces of the alkyl chain of entropic and hydrophobic nature together with H-bonding and the electrostatic interactions of the ionic groups [30]. It should be noted that AK5-6 demonstrated the highest aggregation tendency. To interpret the observed differences in the dye aggregation behavior, Logarithmic Partition coefficients (*LogP*) were calculated (Table 5). Lipophilicity, an important molecular parameter, characterizes the tendency of a molecule to distribute between water and water-immiscible solvent [32–34]. This parameter can be expressed by a volume or cavity term accounting for hydrophobic and dispersion forces, and polarity term determined by electrostatic interactions [32]. Having the highest *LogP* value, AK5-6 with a phenyl ring in N-substitution seems to be most hydrophobic, thereby displaying most pronounced aggregation tendency among the dyes under investigation.

Binding of Cyanine Dyes to Lipid Vesicles

Next step of the study was directed towards the evaluation of possible biological applications of the examined cyanine dyes.

Table 4 Quantum yields of pentamethine cyanine dyes measured in different solvents

Dye	MeOH	DMSO	CH_3CN	DMF	$CHCl_3$
AK5-1	0.10	0.19	0.12	0.09	0.17
AK5-2	0.08	0.18	0.08	0.15	0.30
AK5-3	0.10	0.18	0.11	0.15	0.19
AK5-4	0.07	0.24	0.08	0.12	0.25
AK5-6	0.13	0.28	0.09	0.17	0.22
AK5-8	0.08	0.24	0.09	0.14	0.08
AK5-9	0.10	0.21	0.10	0.17	0.11

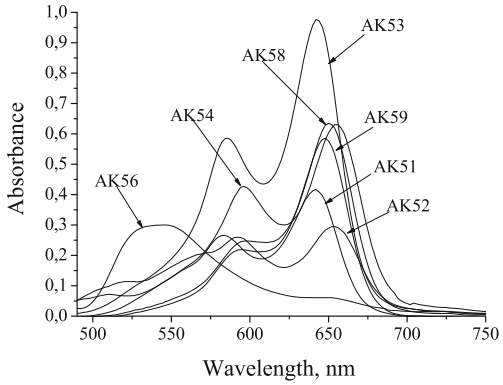

Fig. 2 Absorption spectra of the dyes in buffer. Dye concentrations were 5 μM, 7,3 μM, 7.2 μM, 7.8 μM, 5.6 μM, 4.8 μM and 4 μM for AK5-1, AK5-2, AK5-3, AK5-4, AK5-6, AK5-8 and AK5-9, respectively

Figure 3 shows the representative absorption spectra of pentamethine cyanine dyes in the absence and presence of CL67 lipid vesicles. The changes in these spectra upon lipid addition can be summarized as follows:

i. absorbance of AK5-3, AK5-4, AK5-8 and AK5-9 decreases in the presence of liposomes. The absorption spectrum undergoes changes from 'two-peak' to 'three-peak' form manifesting itself in the appearance of the third well-defined hypsochromic band, suggesting that in a lipid-bound state these dyes are represented by monomers, H-dimers and H-aggregates. The magnitude of the absorbance decrease was more pronounced for the monomeric species, resulting in nearly equal contribution of different dye fractions into the overall spectrum;
ii. the monomeric band of AK5-1 and AK5-2 exhibites significant decrease upon formation of dye-lipid complexes, and the contribution of the aggregated species dominates over the monomeric ones (Fig. 3b). This implies that H-aggregates are the dominating species of AK5-1 and AK5-2 in a lipid-bound state;
iii. association of AK5-6 with the lipid vesicles led to the diminishing of the peak, attributed to the dye H-aggregates (540 nm) and appearance of the new peak around 660 nm, characteristic of the monomer absorption

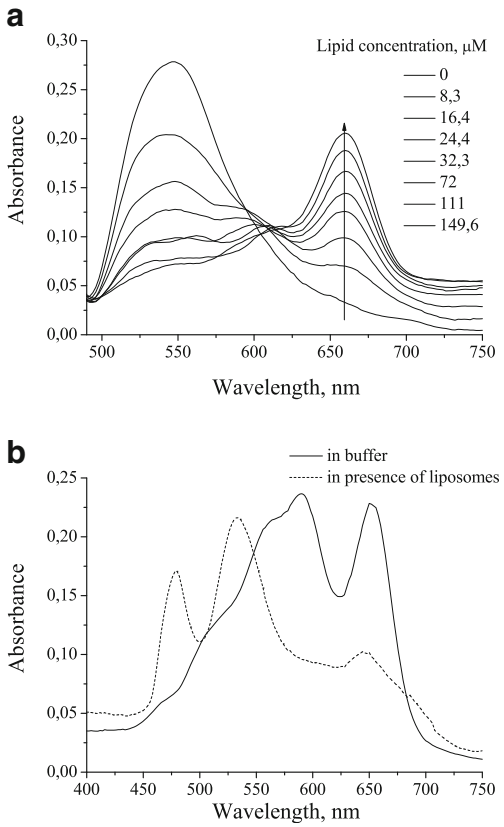

Fig. 3 Absorption spectra of AK5-6 (**a**) and AK5-2 (**b**) recorded in the presence of liposomes. AK5-6 and AK5-2 concentrations were 4.5 μM and 4.3 μM, respectively. Lipid concentration was 81.9 μM

Table 5 Absorption maxima of pentamethine cyanine dyes in buffer and in the presents of liposomes, DNA and BSA

Dye	Buffer*		In liposome		In DNA presence		In BSA presence		[b]LogP
	[*]λ_A^H	λ_A^M	λ_A^H	λ_A^M	λ_A^H	λ_A^M	λ_A^H	λ_A^M	
AK5-1	583, 503	640	583, 521[a]	649	504[a]	640	589, 543	651	2.62
AK5-2	592, 543	654	531[a], 480	644	518[a]	654	543[a], 502	651	2.13
AK5-3	585	642	548, 594[a]	652	585, 539[a]	642	586	640	3.37
AK5-4	596	655	604[a], 563	664	554[a]	655	597, 566	655	2.88
AK5-6	542[a]	653	542	660	542	653	542	653	5.81
AK5-8	594	650	603	660	597	648	600	650	1.53
AK5-9	592	647	601, 555	654	592, 540	647	592	647	1.36

[*] λ_A^H, λ_A^M are absorption wavelength of aggregates maxima and monomeric dye form

[a] The most intensive maximum, in the case that this maximum does not belong to dye monomers

Log P

(Fig. 3a). The observed effect assumes that dye-lipid complexation breaks AK5-6 aggregates, and the dye experiences transition into the monomeric state. Furthermore, absorption spectra of AK5-6 measured at increasing lipid concentration display isosbestic point, indicating the equilibrium between the two main absorbing species – monomers and H-aggregates.

Taken together, these results suggest that transfer of the cyanine dyes into the lipid environment enhances their aggregation propensity. The exception was only AK5-6 which showed the opposite behavior. The aggregation of cyanine dyes is a well-studied process. In an aqueous solution the formation of cyanine aggregates occurs at high fluorophore concentrations. Furthermore, such aggregates are usually unstable and easily destroyed upon heating. The situation changes when the dye is transferred to the low-polarity environment where cyanines self-associate easily even in diluted solutions at room temperature [30]. The molecular basis for such phenomenon lies in the fact that aggregation of the dyes in the low polar solvents, in contrast to highly polar solvents, is controlled not only by the dispersion forces (which govern the stacking orientation of the dye monomers in the aggregate structure), but also by electrostatic interactions [30]. It was postulated that in solvents with high dielectric constant cyanines exist in the form of solvated ions [35]. Upon decreasing the values of dielectric constant, cyanine dyes change their functional state to so-called 'contact ionic pairs'. Further lowering the dielectric constant results in close approaching of these pairs with their concomitant association into the aggregates, stabilized additionally by electrostatic interpair forces. In the case of our systems, it is likely that lipid vesicles not only provide the environment with reduced polarity, but also serve as a template for dye oligomerization. It may be supposed that strong electrostatic lipid-dye interactions ensure the lipid bilayer surface association of the cyanines, increasing thereby their local concentration and eventually promoting the formation of stacked H-aggregates. The proposed scenario is corroborated also by the observation that cyanine dyes were non-fluorescent in the presence of liposomes (when excited near the maximum of monomer adsorption 620 nm). This fact represents the spectroscopic signature of aggregate formation according to excitation coupling theory [36].

In contrast, the results obtained with AK5-6 suggest that this dye reduces its aggregation propensity upon incorporation into the lipid membranes. Presumably, upon exposure to more hydrophobic lipid bilayer, highly organized plane-to-plane arrangement, which is characterized by a broad H-band, is disrupted, thereby favoring the randomized monomer arrangement. Cyanine disaggregation as a result of dye association with biological macromolecules such as DNA [37] and BSA [31] was reported also in other studies and was interpreted as arising from higher strength of interactions between the dye and the macromolecule compared to the coupling between the cyanine monomeric species in the aggregate. Additional arguments in favor of dye disaggregation come from the appearance of fluorescence spectra for AK5-6 in the range 630–750 nm with the maximum at 675 nm (Fig. 4).

Complexation of Pentamethine Cyanines to Bovine Serum Albumin

In the following, the spectral properties of the examined pentamethine cyanine dyes were analyzed upon their binding to bovine serum albumin. Absorption spectra of AK5-3, AK5-6, AK5-8 and AK5-9 in the presence of the protein were featured by two main bands corresponding to monomers and H-aggregates (Table 5). The position of monomer peak was around 640–650 nm while aggregates were the most absorptive at 586, 542, 600 and 592 nm, respectively. Furthermore, BSA addition to the dye solution resulted in 1.3, 1.2, 1.2 and 1.1-fold decrease of monomer and aggregate absorption, respectively, without any modification in the shape of the spectrum. In turn, association of AK5-1 and AK5-4 with BSA was followed by 1.9 and 2.3-fold lowering of the monomer absorbance, respectively, and 1.2-fold decrease in aggregate absorption. In addition, formation of BSA complexes with AK5-1 and AK5-4 led to the appearance of the third blue-shifted shoulder centered at 543 and 566 nm, reflecting the formation of H-aggregates of higher order. Notably, the absorption of aggregate bands was slightly lower compared to monomeric one, suggesting that in the presence of BSA the concentration of dye monomers decreases and the concentration of aggregates increases, but the contribution of these fractions into the overall spectral response is virtually equal. An interesting behavior upon formation of dye-protein complexes was revealed only for AK5-2 (Fig. 5). In the absence of BSA the absorption spectra of this dye has two main bands at 654 (monomers) and 592 nm (H-dimers) coupled with a shoulder at 543 nm (H-aggregates). The binding to BSA provoked 2.3-

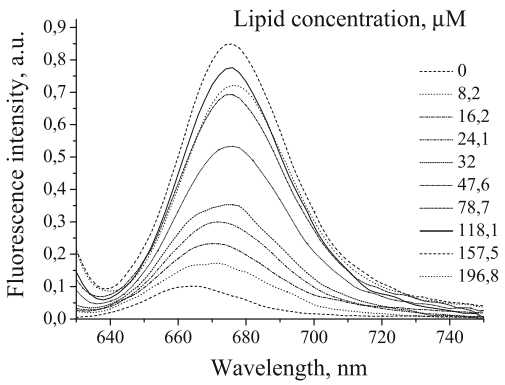

Fig. 4 Emission spectra of pentamethine cyanine dyes in CL67 lipid bilayer. AK5-6 concentration was 1 μM

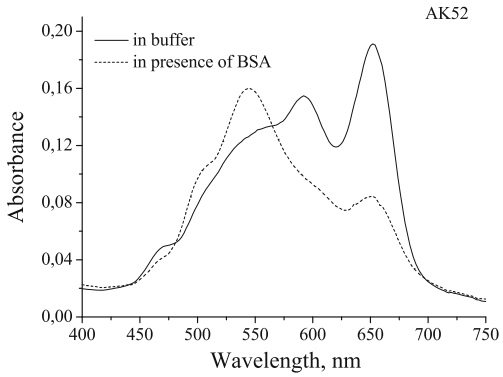

Fig. 5 Absorption spectra of AK5-2 in the presence of bovine serum albumin. AK5-2 concentration was 7 μM. BSA concentration was 6.2 μM

fold drop in monomeric absorption, with almost fully diminishing the dimeric band and 1.2- fold rise in H-aggregate band. Moreover, the contribution of H-aggregate band in the total spectrum was prevailing over the other dye forms. This observation mirrors the ability of BSA to increase the H-aggregation propensity of AK5-2, resulting in the domination of the aggregated dye fraction in protein-bound state.

Association of the Cyanine Dyes with dsDNA

The complexation of pentamethine cyanine dyes with DNA resulted in attenuation of the monomer absorption band (Fig. 6, Table 5). For AK5-1, AK5-2, AK5-3 and AK5-4 the monomer peak almost disappeared and the shift of the aggregate absorption towards the lower wavelengths was observed. Furthermore, this blue-shifted band was found to increase with DNA concentration. These findings suggest the enhancement of dye aggregation in the presence of DNA. The role of DNA as a template for cyanine aggregate growth was also reported in other works [29, 31, 38]. It was postulated that minor groove of nucleic acid provides a favorable environment for cyanine binding and self-assembly. Armitage et al. suggested that DNA-templated aggregation of cyanines is

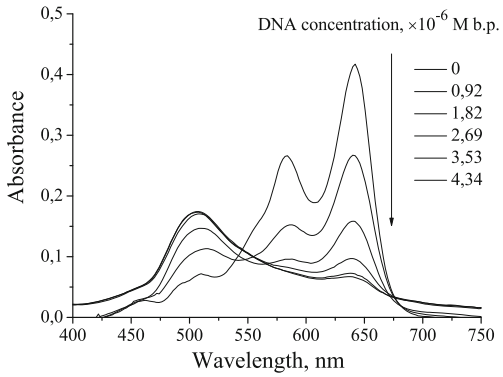

Fig. 6 Absorption spectra of AK5-1 in the presence of DNA. AK5-1 concentration was 4.5 μM. DNA concentration was $1 \cdot 10^{-5}$ M b.p

characterized by two-leveled cooperativity [38]. At the first level association of one monomer molecule with DNA groove facilitates the binding of a second monomer. The origin of this effect lies in unfavorable van der Waals interactions between the planar dye and nonplanar DNA. Thus, association with another monomer and dimer formation will be more optimal. At the second level existing DNA-bound dimer stimulates accumulation of other dimers or *n*-mers nearby. This phenomenon may be explained as follows. The formation of dye dimer in DNA groove is known to widen the groove. Such preopening will induce the association of additional dye dimers or *n*-mers since the binding to the already perturbed groove will require less energy penalty compared to unperturbed one.

Forster Resonance Energy Transfer Between DSP-12 and Cyanine Dyes

From the above results one can conclude that increase in the H-aggregation propensity of pentamethine cyanine dyes under study in the presence of biomacromolecules and lipid membranes (except of the aforementioned particular cases), hinders their application in fluorescence studies, since generally, plane-to-plane H-aggregates are non-fluorescent [39]. Therefore, to get further insights into the interactions of cyanine dyes with biological objects, Forster resonance energy transfer (FRET) between fluorescent probe DSP-12 as a donor and pentamethine cyanines as acceptors was investigated in the presence of liposome, DNA and BSA. As seen in Fig. 7, FRET between membrane-, DNA- or BSA-bound DSP-12 and cyanine dyes manifested itself in the progressive decrease of DSP-12 fluorescence intensity and, accordingly, relative quantum yield, with increasing concentration of pentamethines. The occurrence of FRET can be considered as an additional argument in favor of pentamethine ability to associate with DNA, BSA and model membranes. Presented in Fig. 8a are the relative quantum yields of DSP-12 plotted against the concentration of pentamethines for different types of liposomes. As seen in Fig. 8, the efficiency

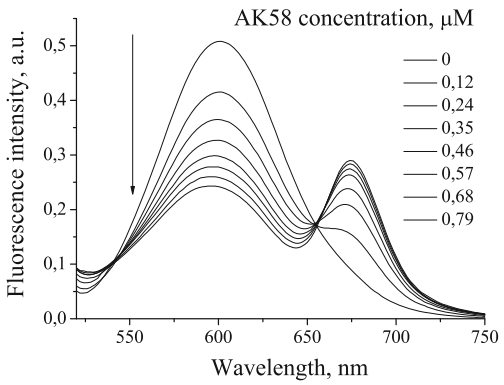

Fig. 7 Emission spectra of DSP-12 in CL11 liposomes recorded at varying concentration of the pentamethine cyanine dye AK5-6. Lipid concentration was 81.9 μM. DSP-12 concentration was 0.4 μM

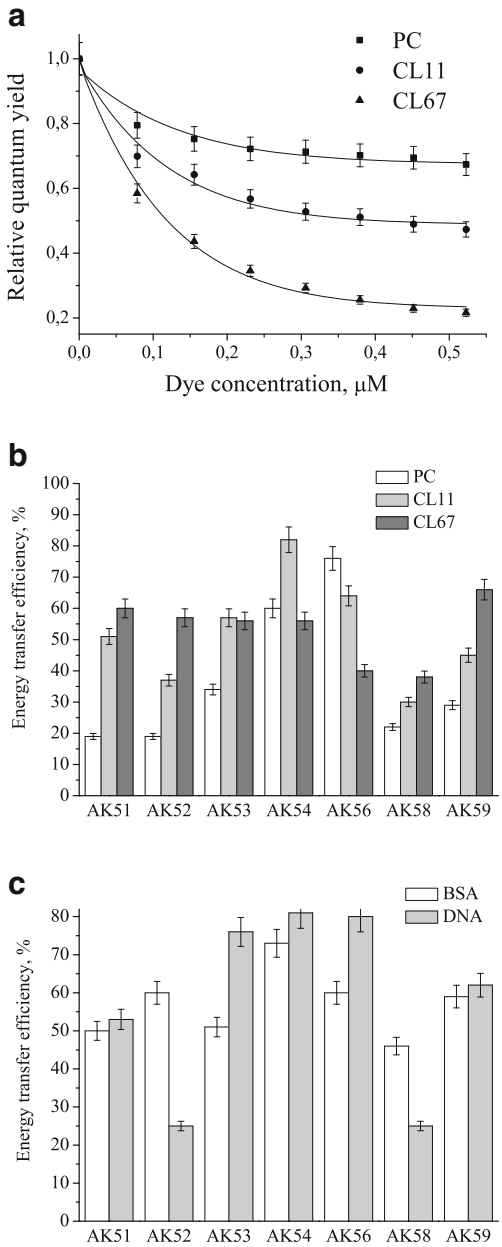

Fig. 8 **a** Relative quantum yield of DSP-12 in the dye-lipid systems as a function of dye concentration in different liposomes. **b** and **c** represent energy transfer efficiency in the presence of liposome, DNA and BSA, measured at the cyanine concentrations 0.24 μM, 0.25 μM and 0.75 μM, respectively. Lipid concentration was 81.9 μM. DSP-12 concentration was 0.4 μM. DNA and BSA concentrations were was $1 \cdot 10^{-5}$ M b.p. and 6.5 μM, respectively

of energy transfer is most pronounced in lipid-containing systems (see Fig. 8). Furthermore, for AK5-1, AK5-2, AK5-8 and AK5-9, energy transfer efficiency exhibits marked dependence on the bilayer content of anionic phospholipid CL, pointing to the predominant role of electrostatic interactions in the membrane partitioning of these probes. Cyanine dye AK5-6 demonstrated the opposite behavior, since the highest energy transfer efficiency was in the presence of pure PC liposomes. The observed tendency is most probably a result of high aggregation propensity of AK5-6. The dye transition into aggregated form, is likely to cause the overlapping of the aggregate peak with DSP-12 emission spectrum, thereby complicating the interpretation of FRET data.

In the case of AK5-3 and AK5-4 ambiguous effects were observed: the initial increase in CL content up to 11 mol% initiated 1.5-fold increase in energy transfer efficiency in comparison with the neat PC bilayer, while further increase in anionic lipid concentration resulted in the drop of energy transfer with the magnitude of this effect being most pronounced for AK5-4. In the BSA-DSP12 system the largest decrease in relative quantum yield of DSP-12 was observed in the presence of pentamethine dyes AK5-2, AK5-4 and AK5-6, whereas in DNA-containing mixtures marked increase in FRET efficiency was caused by all studied dyes except of AK5-2 and AK5-6.

In conclusion, the present study was focused on improved synthesis and spectral characteristics of a series of pentamethine cyanine dyes. The dyes under study were found to aggregate in different solvents with the extent of aggregation being dependent on solvent polarity. Based on the results of absorption studies, it was concluded that cyanine dyes are capable of associating with nucleic acids, proteins and biomembranes and this process is accompanied by the changes in dye aggregation potential. The recovered pronounced changes in spectral responses of AK5-1 – AK5-4 upon association with DNA allowed us to recommend these dyes for sensitive detection of nucleic acids.

References

1. Pauli J, Vag T, Haag R, Spieles M, Wenzel M, Kaiser W, Resch-Genger U, Hilger I (2009) An in vitro characterization study of new near infrared dyes for molecular imaging. Eur J Med Chem 44: 3496–3503
2. Ebert B, Riefke B, Sukowski U, Licha K (2011) Cyanine dyes as contrast agents for near-infrared imaging in vivo: acute tolerance, pharmacokinetics and fluorescence imaging. J Biomed Opt 16(6): 060030–060039
3. Lidzey D, Bradley D, Virgili T, Armitage A, Skolnick H, Walker S (1999) Room temperature polariton emission from strongly coupled organic semiconductor microcavities. Phys Rev Lett 82(16):3316–3319
4. Jenatsch S, Geiger T, Heier J, Kirsch C, Nuesch F, Paracchino A, Rentsch D, Ruhstaller B, Veron A, Hany R (2015) Influence of chemically p-type doped active organic semiconductor on the film thickness versus performance trend in cyanine/C_{60} bilayer solar cells. Sci Technol Adv Mater 16:0350030–0350039
5. Czerney P, Graneb G, Birckner E, Vollmer F, Rettig W (1995) Molecular engineering of cyanine-type fluorescent and laser dyes. J Photochem Photobiol A Chem 89:31–36
6. Castro F, Faes A, Geiger T, Graeff C, Nagel N, Nuesch F, Hany R (2006) On the use of cyanine dyes as low-band gap materials in bulk heterojunction photovoltaic devices. Synth Met 156:973–978

7. Wu W, Hua J, Jin Yi, Zhan W, tian H (2008) Protovoltaic Properties of Tree new Cyanine Dyes for dye-Sensitized Solar Cells Photochem Photobiol Sci 7:63–68.
8. Chatterju S, Gottschalk P, Davis P, Schuster G (1988) Electron-transfer reactions in cyanine borate ion pairs: photopolymerization initiators sensitive to visible light. J Am Chem Soc 110(7):2326–2328
9. Ja K, Zasada M, Paczkowski J (2007) Photopolymerization reaction initiated by a visible light photoinitiating system: cyanine dye/borate salt/1,3,5,-triazine. J Polym Sci Part A: Polym Chem 45(16): 3626–3636
10. Markova L, Malinovskii V, Patsenker L, Haner R (2013) J-vs. H-type assembly: penthamethine cyanine (Cy5) as a near-IR chiroptical reporter. Chem Commun 49:5298–5300
11. Nanjunda R, Owens E, Mickelson L, Dost T, Stroeva K, Huynh H, Germann M, Henary M, Wilson W (2013) Selective G-quadruplex DNA recognition by a new class of desined cyanines. Molecules 18:13588–13607
12. Kaloyanova S, Trusova V, Gorbenko G, Deligeorgiev T (2011) Synthesis and fluorescence characterization of novel asymmetric cyanine dyes for DNA detection. J Photochem Photobiol A 217: 147–156
13. Guralchuk G, Sorokin A, Katrunov I, Yefimova S, Lebedenko A, Yu M, Yarmoluk S (2007) Specificity of cyanine dye L-21 aggregation in solution witrh nucleic acids. J Fluoresc 17:370–376
14. Mishra A, Behera R, Behera P, Mishra B, Behera G (2000) Cyanines during the 1990s: a review. Chem Rev 100:1973–2011
15. Kricka L (2002) Stains, labels and detection strategies for nucleic acids assays. Ann Clin Biochem 39(2):114–129
16. Biver T, Boggioni A, Secco F, Turriani E, Venturini S, Yarmoluk S (2007) Influence of cyanine dye structure on self-aggregation and interaction with nucleic acids: a kinetic approach to TO and BO binding. Arch Biochem Biophys 465:90–100
17. Davidson Y, Gunn B, Soper S (1996) Spectroscopic and binding properties of near-infrared tricarbocyanine dyes to double-stranded DNA. Appl Spectrosc 50(2):211–221
18. Rye H, Yue S, Wemmer D, Quesada M, Haughland R, Mathies R, Glazer A (1992) Stable fluorescence complexes of double-stranded DNA with bis-intercalating asymmetric cyanine dyes: properties and application. Nucleic Acids Rev 20:2803–2812
19. Volkova K, Kovalska V, Balanda A, Losytskyy M, Colub A, Vermeij R, Subramaniam V, Tolmachev O, Yarmoluk S (2008) Specific fluorescent detection of fibrillar alpha-synuclein using mono- and trimethine cyanine dyes. Bioorg Med Chem 16:1452–1459
20. Kovalska V, Losytskyy M, Tolmachev O, Yu S, Segers-Nolten G, Subramaniam V, YArmoluk S (2012) Tri- and pentamethine cyanine dyes for fluorescence detection of α-synuclein oligomeric aggregates. Is Missing the Journal 22(6):1441–1448
21. Sovenyhazy K, Bordelon J, Petty J (2003) Spectroscopic studies pf the multiple binding modes of a trinethine-bridged cyanine dye with DNA. Nucleic Acids Res 31(10):2561–2569
22. Kovalska V, Tokar V, Losytskyy M, Deligeorgiev T, Vassilev A, Gadjev N, Drexhage K, Yarmoluk S (2006) Studies of monomeric and homodimeric oxazolo[4,5-b]pyridinium cyanine dyes as fluorescent probes for nucleic acids visualization. J Biochem Biophys Methods 68(3):155–165
23. Puyol M, Encinas C, Rivera L, Miltsov S, Alonso J (2007) Characterisation of new norcyanine dyes and their application as pH chromoionophores in optical sensors. Dyes Pigments 73:383–389
24. Zhang Z, Achilefu S (2005) Design, synthesis and evaluation of near-infrared fluorescent pH indicators in a physiologically relevant range. Chem Commun:5887–5889
25. Guo Z, Park S, Yoon J, Skin I (2014) Recent progress in the development of near-infrared fluorescent probes for bioimaging applications. Chem Soc Rev 43(1):16–29
26. Luo S, Zhang E, Yo S, Cheng T, Shi C (2011) A review of NIR dyes in cancer targeting and imaging. Biomaterials 32:7127–7138
27. Bartlett G (1959) Phosphorus assay in column chromatography. J Biol Chem 234:466–468
28. Bulychev A, Verchoturov V, Gulaev B (1988) Current methods of biophysical studies. Vyschaya shkola, Moscow
29. Caroff A, Litzinger E, Connor R, Fishman I, Armitage B (2002) Helical aggregation of cyanine dyes on DNA templates: effect of dye structure on formation of homo- and heteroaggregates. Langmuir 18:6330–6337
30. Kirstein S, Daehne S (2006) J-aggregates of amphiphilic cyanine dyes; self-organization of artificial light harvesting complexes. Int J Photogr 2006:1–21
31. Losytskyy M, Volkova K, Kovalska V, Makovenko I, Yu S, Tolmachev O, Yarmoluk S (2005) Fluorescence properties of pentamethine cyanine dyes with cyclopentene and cyclohexene group in presence of biological molecules. J Fluoresc 15(6):849–857
32. Balen G, Martinet C, Caron G, Bouchard G, Reist M, Carrupt P, Fruttero R, Gasco A, Testa B (2004) Liposome/water lipophilicity: methods, information content, and pharmaceutical applications. Med Res Rev 3:299–324
33. Ahsan M, Samy J, Khalilullah H, Nomani M, Saraswat P, Gaur R, Singh A (2011) Molecular properties prediction and synthesis of novel 1, 3, 4-oxadiazole analogues as potent antimicrobial and antitubercular agents. Bioorg Med Chem Lett 21(24):7246–7250
34. Irwin J, Shoichet B (2005) ZINC-a free database of commercially available compounds for virtual screening. J Chem Inf Model 45: 177–182
35. Ishchenko A Structure and spectral-luminescent properties of polymethine dyes. Russ Chem Rev 60:865–884.
36. Kasha M (1963) Energy transfer mechanism and the molecular exciton model for molecular aggregate. Radiat Res 20:55–71
37. Ogul'chansky T, Yaschuk V, Losytskyy M, Kocheshev I, Yarmoluk S (2000) Interaction of cyanine dyes with nucleic acids. XVII towards an aggregation of cyanine dyes in solutions as a factor facilitating nucleic acid detection. Spectrochim Acta Part A 56:805–814
38. Hannah K, Armitage DNA-templated assembly of helical cyanine dye aggregates: a supramolecular chain polymerization. Acc Chem Res 37:845–853.
39. Kasha M, Rawls H, El-Bayoumi M The exciton model in molecular spectroscopy Pure Appl Chem 11:372–392.